JOURNAL OF MATERIALS SCIENCE 23 (1988) 699–706

Structure of chemically vapour deposited silicon carbide for coated fuel particles

KAZUO MINATO, KOUSAKU FUKUDA
Department of Fuels and Materials Research, Japan Atomic Energy Research Institute, Tokai-mura, Ibaraki-ken, Japan

The silicon carbide coating layers prepared under various conditions were examined by density measurement, X-ray diffractometry, and optical and scanning electron microscopies in order to clarify the relation between deposition conditions and structure of the coating layers. It was found that the deposition temperature was the main parameter affecting the content of free silicon, density, crystallite size and lattice distortion, and microstructure. The dependence of these properties on the coating rate and the composition of fluidizing gas was not observed clearly. Free silicon was co-deposited with β-SiC at temperatures lower than 1400 to 1500° C, and the content of free silicon increased with decreasing deposition temperature. The density of the layers without free silicon was more than 3.210 Mg m^{-3} and the density decreased with increasing content of free silicon. Crystallite size increased with deposition temperature and lattice distortion decreased with increasing deposition temperature. The outer surfaces of the layers without free silicon consisted of large interlocked grains, whereas those of the layers with free silicon showed a cauliflower-like structure of which the apparent grain size was small.

1. Introduction

Chemical vapour deposition of silicon carbide (SiC) has been applied to Triso-coated fuel particles for high-temperature gas-cooled reactors (HTGR). The Triso-coated fuel particle, which is less than 1 mm in diameter, consists of a microspherical fuel kernel surrounded by four layers: porous pyrolytic carbon (PyC), dense PyC, SiC, and dense PyC. The function of these layers is to retain fission products within the particle. In particular the SiC layer acts as a diffusion barrier to metallic fission products and a miniature pressure vessel for the particle.

As far as the SiC properties are concerned, the following behaviour has been studied in the coated fuel particles. The experimental results of Förthmann *et al.* [1] and Bullock [2] suggested that the diffusion behaviour of fission products in the SiC layer depends on the microstructure of the layer. The reaction of the SiC layer with fission-product palladium during irradiation was observed [3–6]; its reaction rate may be affected by the deposition conditions of the layer [4, 5]. It was also suggested that the thermal degradation of the SiC layer during irradiation was partly attributed to the content of free silicon in the layer [7]. Since the irradiation behaviour of the SiC is thus affected strongly by its properties depending on the deposition conditions, characterization of the SiC layers is of importance from a viewpoint of the irradiation performance.

The microstructure and properties of the SiC layers have been studied as a function of deposition conditions [8–13], but these results were not completely related to the irradiation behaviour.

In the present study, as the first step, the SiC layers prepared under various conditions were characterized by density measurement, X-ray diffractometry, and optical and scanning electron microscopy in order to clarify the relation between deposition conditions and the structure of the deposits. The relation between deposition conditions and irradiation behaviour of these layers will be discussed elsewhere [14].

2. Experimental procedure

2.1. Materials

Silicon carbide coating layers examined in the present study were chemically vapour deposited on PyC-coated fuel particles in a fluidized-bed coater under various conditions. Methyltrichlorosilane (CH_3SiCl_3, MTS) was used as a reactant with a fluidizing gas of hydrogen (H_2) or a mixture of hydrogen and argon (Ar). The deposition temperature ranged between 1700 and 1150° C (1973 and 1423 K), and the deposition rate between 1.10 and 0.08 μm min^{-1}. The deposition temperature referred to the temperature measured at the inner surface of the coater during deposition. The deposition rate was defined as the thickness of the coating divided by the coating time. Deposition conditions of the materials are listed in Table I. Details of the deposition apparatus and conditions have been described elsewhere [15].

2.2. Density measurement

The SiC samples for density measurement were prepared by crushing SiC-coated fuel particles and collecting fragments of the coatings. Since these

0022–2461/88 $03.00 + .12

TABLE I Coating conditions of the deposits

Run No.	Bed temp. (°C)	Flow rate ($ml\,min^{-1}$)		$(H_2 + Ar)/MTS$	Coating rate ($\mu m\,min^{-1}$)	Coating thickness (μm)	Density ($Mg\,m^{-3}$)
		Argon	H_2				
H1024	1700	0	7000	239	1.10	55	3.216
H0612	1700	0	7000	357	0.66	53	3.215
H0907	1700	0	7000	504	0.56	50	3.217
H0918	1700	0	7000	837	0.25	30	3.216
H1022	1600	0	7400	304	0.88	53	3.216
H0625	1600	0	7400	378	0.71	57	3.217
H0709	1600	0	7400	533	0.53	37	3.212
H0703	1600	0	7400	885	0.33	30	3.213
H1106	1500	0	8600	294	0.88	35	3.141
H0619	1500	0	7800	398	0.66	33	3.211
H0710	1500	0	7800	562	0.48	25	3.210
H0919	1500	0	8600	1028	0.22	35	3.209
H1113	1400	0	8600	294	0.75	45	2.923
H0626	1400	0	7800	398	0.56	45	2.980
H0911	1400	0	7800	562	0.36	25	3.061
H0912	1400	0	8600	1028	0.21	14	2.938
H0614	1300	0	8000	409	0.63	50	2.903
H0306	1200	0	9400	479	0.29	23	2.626
H0321	1150	0	9400	479	0.08	9	2.477
M1213	1600	1750	1750	252	0.43	32	3.214
M1219	1500	1750	1750	252	0.39	35	3.213
M1221	1400	1750	1750	252	0.36	30	3.186
M1222	1300	1750	1750	252	0.33	30	3.033
M0311	1200	1750	1750	252	0.26	31	2.676
M0322	1150	1750	1750	252	0.17	20	2.557
M1227	1600	2250	750	251	0.44	24	3.214
M1101	1500	2250	750	251	0.43	34	3.217
M1029	1400	2250	750	251	0.36	32	3.213
M1223	1300	2250	750	251	0.30	33	3.118
M1031	1200	2250	750	251	0.25	28	2.772
M1030	1150	2250	750	251	0.21	25	2.630

coatings consisted of PyC and SiC, the fragments were heated at 800° C in air to burn off PyC.

The density of the SiC fragments were measured by the sink–float technique with use of methylene iodide (CH_2I_2) and benzene (C_6H_6).

2.3. X-ray diffraction

Fragments of SiC, prepared in the same manner as described above, were powdered and analysed by X-ray diffractometry. The content of free silicon was determined with the use of a calibration curve.

Crystallite size and lattice distortion were evaluated from the breadths of the diffraction line profiles. Observed line profiles were corrected in terms of Lorentz and polarization factors, and then $K\alpha_1$ and $K\alpha_2$ line profiles were separated by the Rachinger method [16]. When the shape of the pure, observed, and instrumental line profiles is Gaussian, the pure line profile is obtained by the equation

$$\beta^2 + b^2 = B^2 \quad (1)$$

where β, b and B are the integral breadths of the pure, instrumental and observed line profiles, respectively [17]. The instrumental line profiles were determined with the use of annealed silicon powder. Broadening of the pure line profile is caused by the effects of crystallite size and lattice distortion. When the shape of the two contributing line profiles is Gaussian, the crystallite size and lattice distortion are given by

$$\left(\beta \frac{\cos\theta}{\lambda}\right)^2 = \left(\frac{1}{L}\right)^2 + \left(\frac{4e \sin\theta}{\lambda}\right)^2 \quad (2)$$

where θ is the Bragg angle, λ the wavelength of X-rays, L the crystallite size and e the lattice distortion [17]. If at least two profiles are measured, one can obtain L and e by plotting $(\beta \cos\theta/\lambda)^2$ as a function of $(\sin\theta/\lambda)^2$.

2.4. Optical and scanning electron microscopy

The SiC-coated particles were polished to the mid-plane and observed by an optical microscope. The polished SiC layers were then etched electrolytically. Etching was carried out in the two steps [12]. In the first step an electrolyte of 4 g potassium dicromate ($K_2Cr_2O_7$) in 100 ml phosphoric acid (H_3PO_4) was used and the SiC layers were etched for 20 to 30 sec at 15 V. In the second step the surfaces of the SiC layers were washed with 20% hydrofluoric acid (HF) and then etched with a solution of 10 g oxalic acid ($C_2H_2O_4 \cdot 2H_2O$) in 100 ml water for about 30 sec at 15 V.

Fracture and outer surfaces of the SiC layers were observed with a scanning electron microscope (SEM).

3. Results and discussion

3.1. Density and chemical composition

The chemical composition of the coatings analysed by X-ray diffraction was β-SiC or (β-SiC + Si)

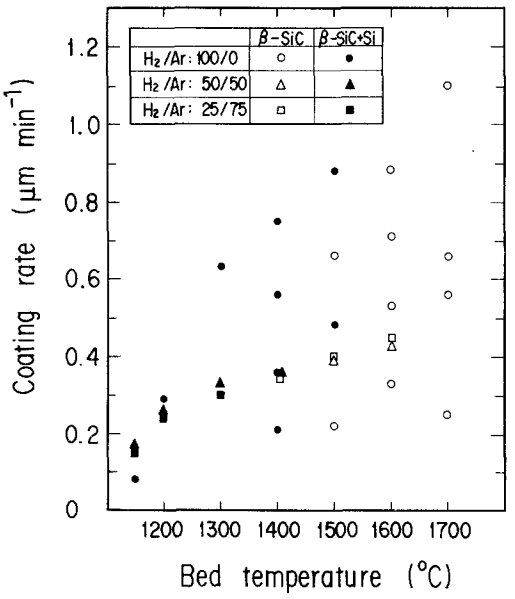

Figure 1 Compositions of the deposits determined by X-ray diffractometry as a function of the deposition conditions.

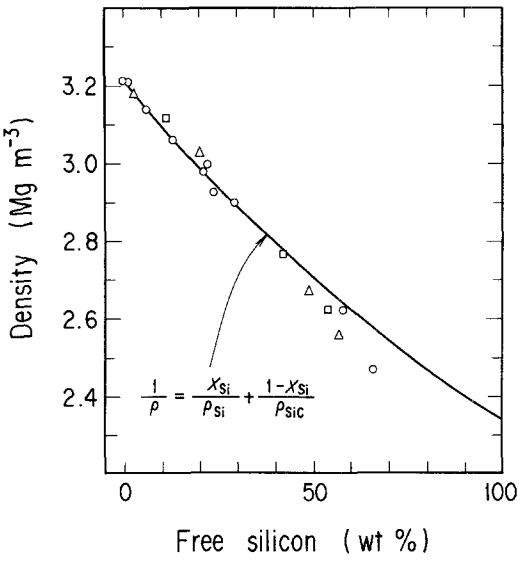

Figure 3 Density of the deposits as a function of the content of free silicon. ϱ denotes the density and X_{Si} the content of free silicon in weight fraction. H_2/Ar = (○) 100/0, (△) 50/50, (□) 25/75.

depending on the deposition conditions. Fig. 1 shows the chemical composition as a function of the coating rate and the bed temperature. When the bed temperature was higher than 1600° C (1873 K) the deposits were β-SiC. Free silicon was included in the deposits at temperatures lower than around 1400 to 1500° C (1673 to 1773 K). The content of free silicon increased with decreasing bed temperature. The effect of the coating rate on the chemical composition was not clear.

Co-deposition of free silicon with β-SiC was also observed in other work [9, 18–21] when the deposition temperature was lower than 1400° C. The mechanism of deposition of free silicon has been discussed in terms of thermodynamics and chemical kinetics [15].

The relation between the density and the bed temperature is shown in Fig. 2. The density of the coatings deposited at temperatures higher than 1500° C (1773 K) is near the theoretical value for SiC (3.217 Mg m^{-3}) [8] and almost constant. When the bed temperature is lower than 1500° C (1773 K), the density decreases with the bed temperature. It can be seen in Fig. 2 that the density slightly depends on the composition of the fluidizing gas; when the bed temperature is fixed, the larger the content of hydrogen is, the smaller is the density. This result may be attributed to temperature profile changes in the fluidized-bed coater. A relation between the density and the coating rate was not clearly observed.

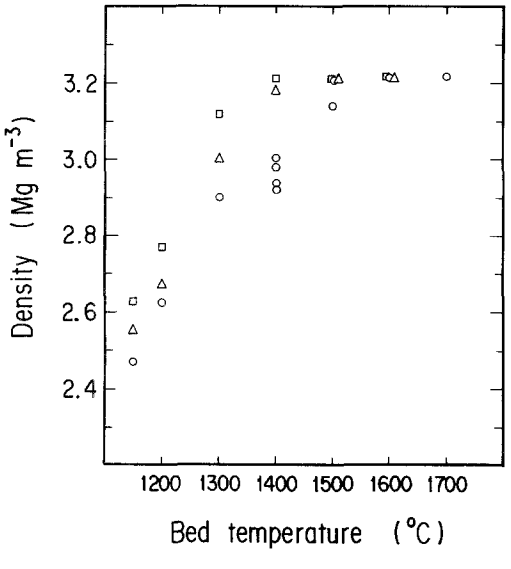

Figure 2 Density of the deposits as a function of the bed temperature. H_2/Ar = (○) 100/0, (△) 50/50, (□) 25/75.

The coating density is plotted as a function of the content of free silicon in Fig. 3. If the deposits are a mixture of β-SiC and silicon crystals without pores, the density of the mixture is given by

$$\frac{1}{\varrho} = \frac{X_{Si}}{\varrho_{Si}} + \frac{1 - X_{Si}}{\varrho_{SiC}} \quad (3)$$

where ϱ is the density of the mixture, X_{Si} the content of free silicon in weight fraction, ϱ_{Si} the theoretical density of silicon crystals and ϱ_{SiC} the theoretical density of β-SiC. The density of the deposits with lower than about 40 wt % free silicon agreed with Equation 3, whereas the density was smaller than the calculated value at the higher free silicon contents. This means that at lower free silicon contents the density decrease was mainly attributed to the content of free silicon, and that the pores as well as the free silicon affected the decrease in density at the higher free silicon contents.

3.2. Crystallite size and lattice distortion

The crystallite size and lattice distortion of the SiC coatings determined by X-ray diffractometry are presented in Fig. 4 as typical results, where the best straight lines are drawn through all the data points. According to Equation 2, the Y-axis intersection of the line indicates $(1/L)^2$ and the slope of the line $(4e)^2$. It can be seen in Fig. 4 that crystallite size and lattice distortion depend on crystallographic directions: the crystallite size and lattice distortion in the [1 0 0] direction (L_{100} and e_{100}) evaluated by the (2 0 0) and (4 0 0) reflections are different from those in the [1 1 1] direction (L_{111} and e_{111}) evaluated by the (1 1 1) and (2 2 2)

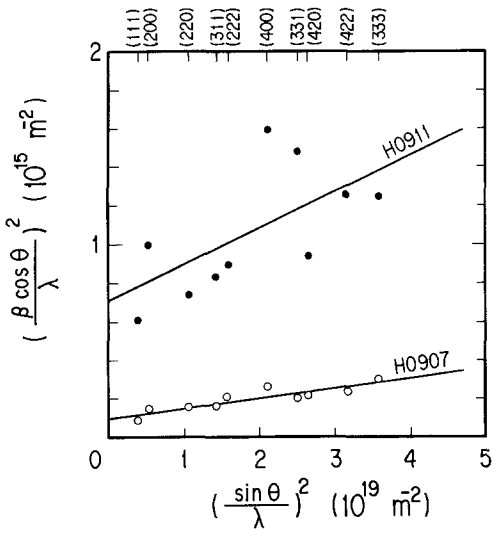

Figure 4 Crystallite size and lattice distortion analysis by X-ray diffraction. β is the integral breadth of the pure line profile, θ the Bragg angle and λ the wavelength of X-rays.

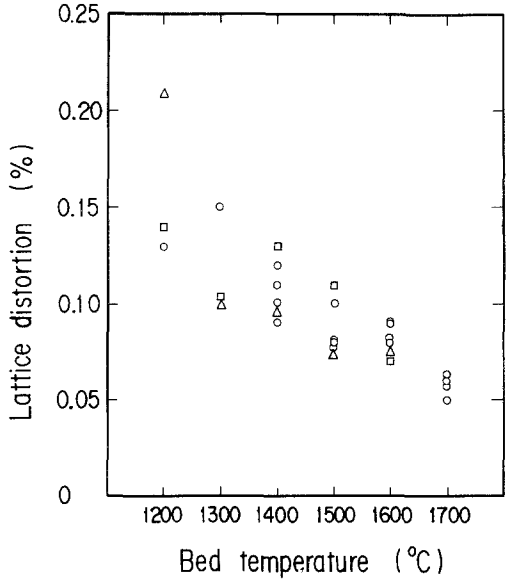

Figure 6 Lattice distortion of the SiC coating layers as a function of the bed temperature. H_2/Ar = (○) 100/0, (△) 50/50, (□) 25/75.

reflections. Although anisotropy was observed, the ratios L_{100}/L_{111} and e_{100}/e_{111} were almost constant in all the deposits studied. The data from all the measured reflections were, therefore, used to determine the mean size and distortion parameters in the present study.

The relation between the crystallite size of the deposits and the deposition temperature is shown in Fig. 5. The crystallite size increases with deposition temperature regardless of the fluidizing gas composition. The crystallite size of SiC deposited at 1200° C (1473 K) is about 10 nm, whereas for that deposited at 1700° C (1973 K) it is about 100 nm. Lattice distortion of the SiC coatings is also dependent on the deposition temperature. As seen in Fig. 6, the lattice distortion decreases with increasing bed temperature. A dependence of lattice distortion on the fluidizing gas composition was not seen. Effects of the coating rate on the crystallite size and lattice distortion were not clearly observed.

The dependence of crystallite size and lattice distortion on the deposition temperature can be explained qualitatively as follows: at high deposition temperatures, high mobility of individual atoms over the crystal surface resulted in the formation of large crystallites with small lattice distortion, whereas low surface mobility of atoms led to small crystallites with large lattice distortion at low deposition temperatures [22]. Holub [21] has also observed the same dependence of crystallite size and lattice distortion on the deposition temperature.

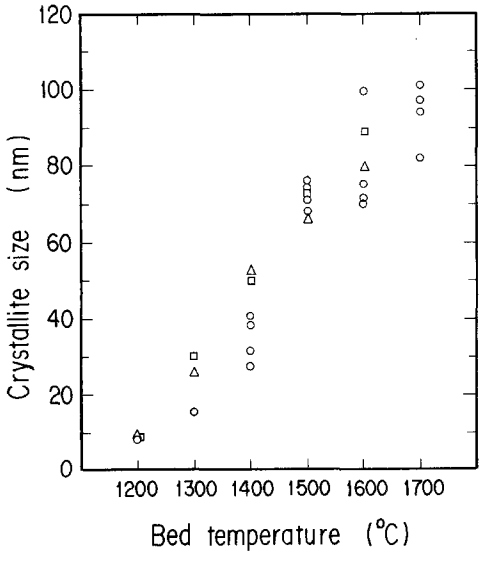

Figure 5 Crystallite size of the SiC coating layers as a function of the bed temperature. H_2/Ar = (○) 100/0, (△) 50/50, (□) 25/75.

3.3. Texture and morphology

Optical micrographs of a polished section of the SiC layers deposited in H_2 are shown in Fig. 7. The SiC layers deposited at 1400° C (1673 K), which contain free silicon, show two phases: β-SiC and silicon. Free silicon is seen as small white spots. Growth cones [22] were observed in the deposits prepared at 1300 and 1400° C (1573 and 1673 K). The spots of free silicon are larger in the coating layers deposited at 1500° C (1773 K), whereas white spots are not seen in the deposits prepared at 1600 to 1700° C (1873 to 1973 K).

Etched sections of the coating layers are presented in Fig. 8. It is seen in the figure that the apparent grain size increases with deposition temperature. These results showed the same tendency as the results of crystallite size analysis. White spots in Fig. 8a are the same as those seen in Fig. 7b. Although the densities of the coating layers presented in Figs 8b to e are nearly the same (3.211 to 3.216 $Mg\,m^{-3}$), the etched structures are quite different from each other.

Fracture surfaces of the coating layers observed by SEM are shown in Fig. 9. These coating layers are of the same kind as those presented in Fig. 7. It is seen again in Fig. 9 that the apparent grain size increases with deposition temperature.

Scanning electron micrographs of the outer surfaces of SiC layers deposited in H_2 are presented in Fig. 10 as a function of deposition conditions. It is seen in the figure that the coating layers deposited at 1400° C (1673 K) show a cauliflower-like structure [13], which may result from growth cones, and the apparent grain size is small. The structure of the outer surface gradually changes with deposition temperature. When the

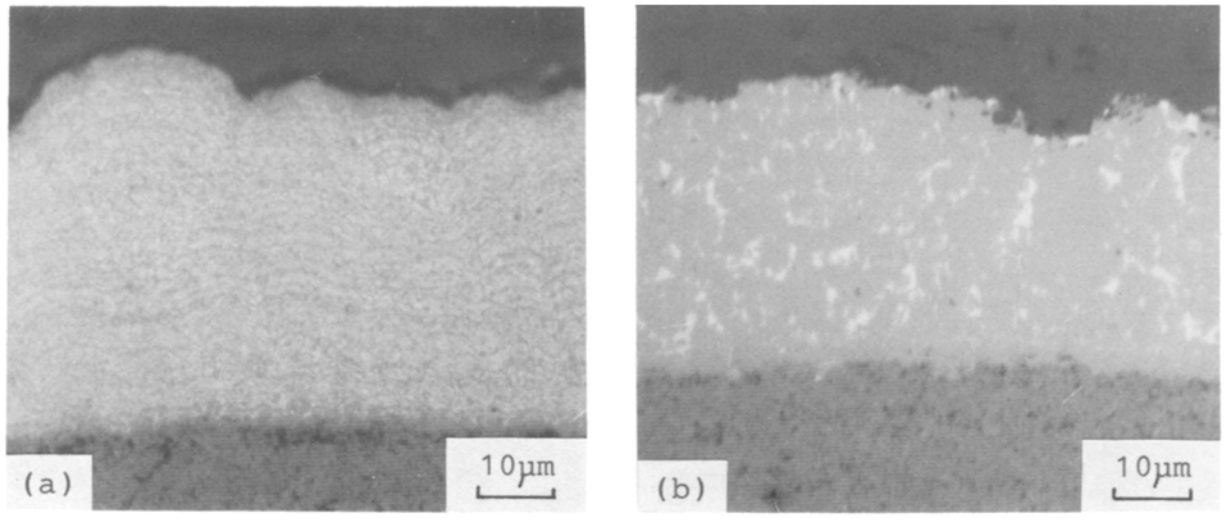

Figure 7 Optical micrographs of polished sections of the SiC coating layers deposited at (a) 1400° C (H1113), (b) 1500° C (H1106) and (c) 1600° C (H1022).

deposition temperature is 1700° C (1973 K), the outer surface consists of large interlocked grains. An effect of coating rate is not seen clearly on the outer surface structure.

The structure of etched, fracture and outer surfaces of the coating layers deposited in the H_2–Ar–MTS system resembled that of the coating layers deposited in the H_2–MTS system. The relation between the structure of the outer surface and coating conditions is shown in Fig. 11, where the ratio $(H_2 + Ar)$/MTS and the coating rate are almost constant. The structure also depends strongly on the bed temperature. When the ratio of gas flow rate $Ar/(Ar + H_2)$ is changed from 50 to 75%, the outer surface structure seems not to be influenced.

4. Conclusions

The SiC coating layers prepared under various conditions were examined by density measurement, X-ray diffractometry, and optical and scanning electron microscopies. The following relations were found between deposition conditions and structure of the SiC layers:

1. Deposition temperature was the main parameter affecting the content of free silicon, density, crystallite size and lattice distortion, and microstructure. Effects of coating rate and $Ar/(Ar + H_2)$ ratio were not observed clearly in the range studied.

2. Free silicon was co-deposited with β-SiC at temperatures lower than 1400 to 1500° C (1673 to

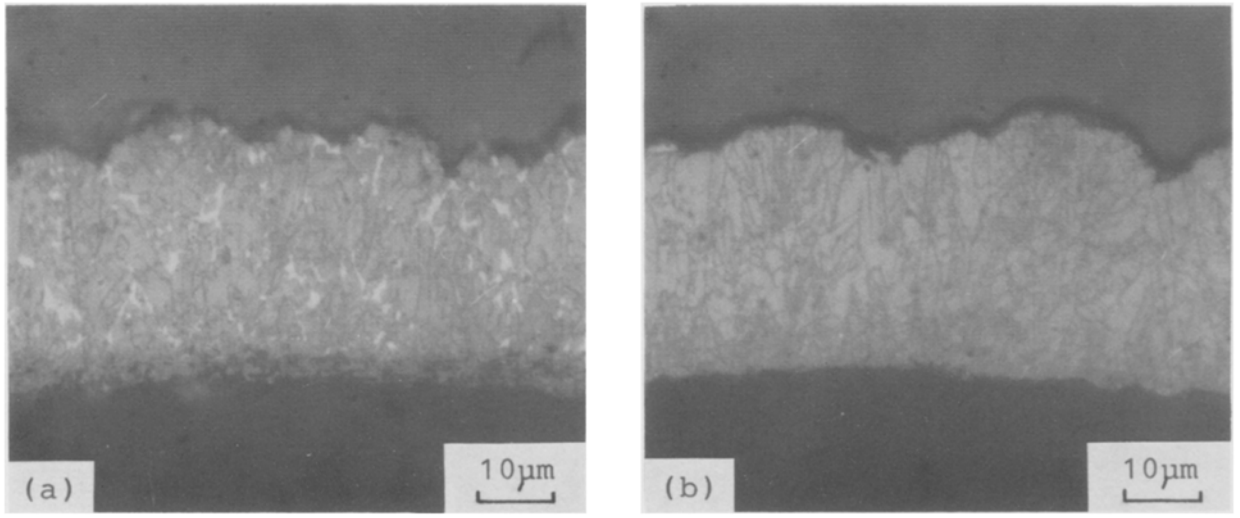

Figure 8 Optical micrographs of etched sections of the SiC coating layers deposited at (a) 1500° C (H1106), (b) 1500° C (H0619), (c) 1600° C (H1022), (d) 1700° C (H0612) and (e) 1700° C (H1024).

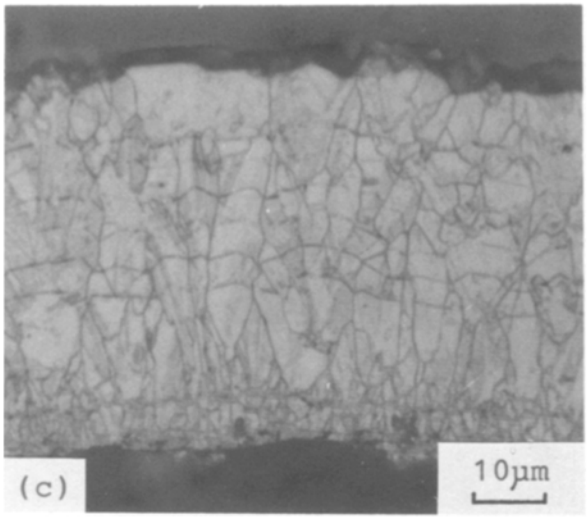

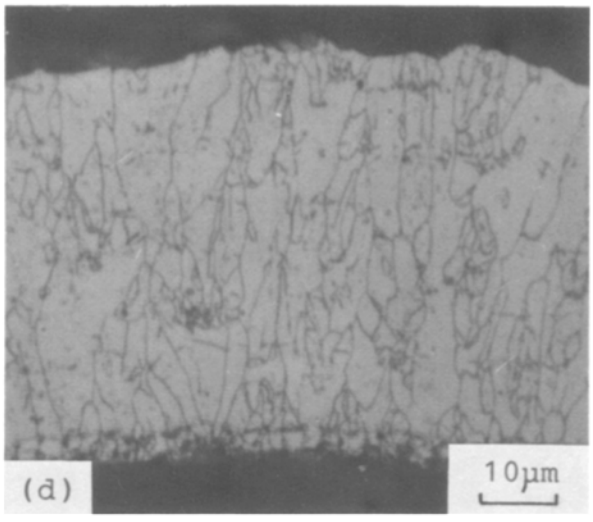

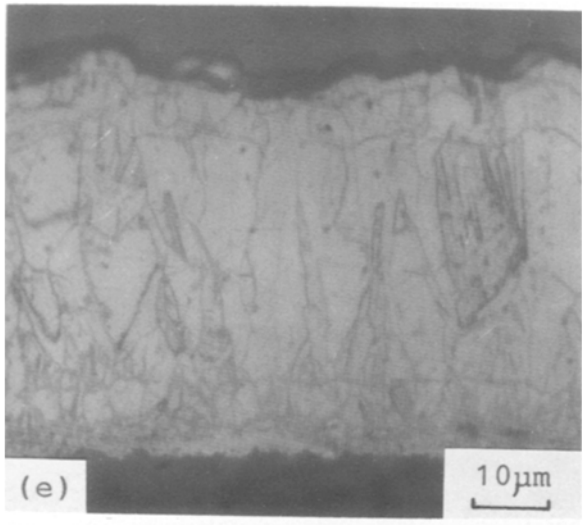

Figure 8 Continued.

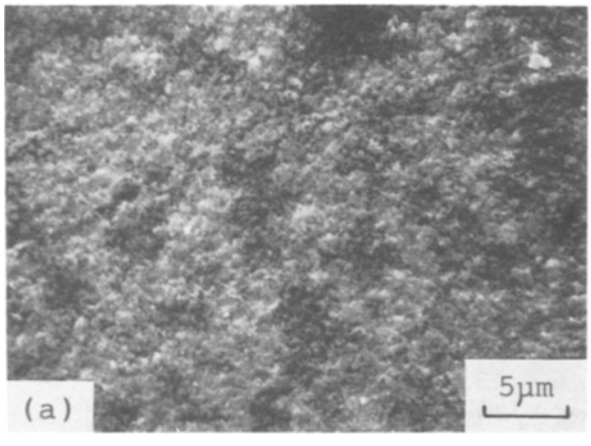

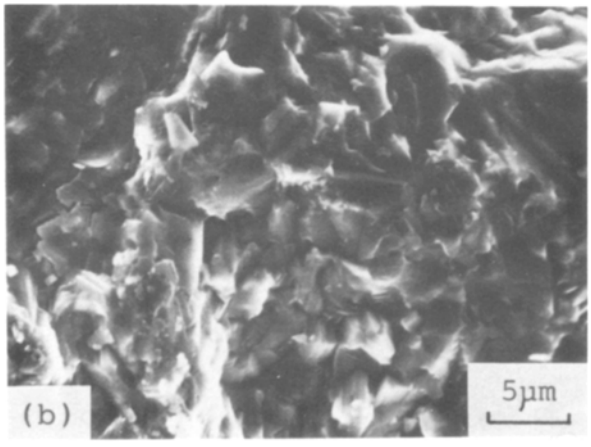

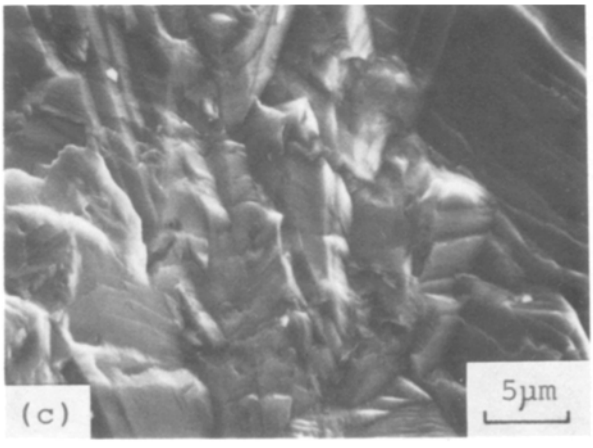

Figure 9 Scanning electron micrographs of the fracture surfaces of SiC coating layers deposited at (a) 1400° C (H1113), (b) 1500° C (H1106) and (c) 1600° C (H1022).

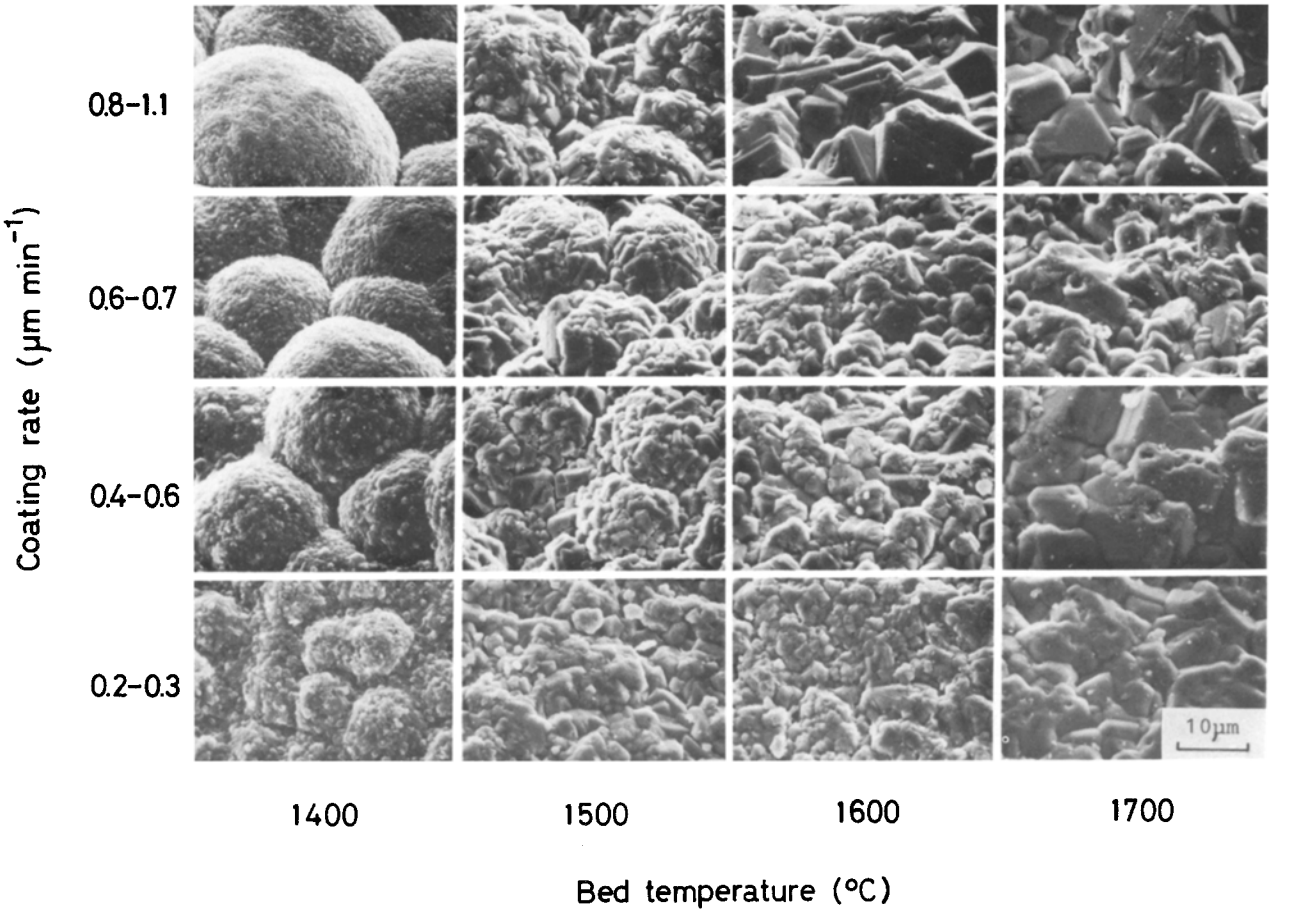

Figure 10 Scanning electron micrographs of the outer surfaces of the SiC coating layers deposited in the H_2–MTS system.

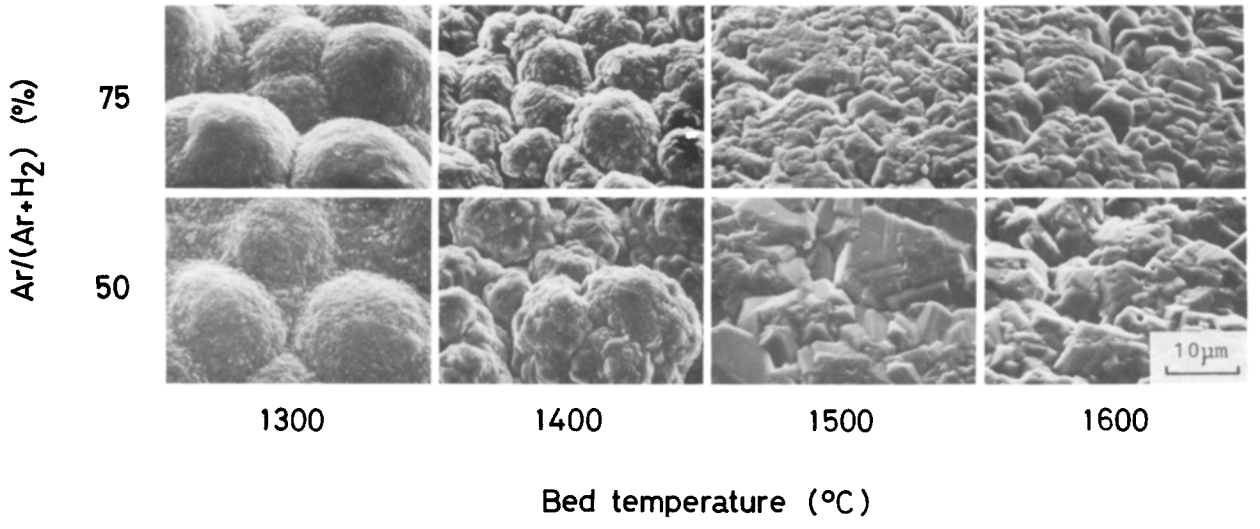

Figure 11 Scanning electron micrographs of the outer surfaces of the SiC coating layers deposited in the H_2–Ar–MTS system.

1773 K). The content of free silicon increased with decreasing deposition temperature.

3. The density of the layers without free silicon was more than 3.210 $Mg\,m^{-3}$, and the density decreased with increasing content of free silicon.

4. Crystallite size increased with deposition temperature and lattice distortion decreased with increasing deposition temperature.

5. The outer surface of the layers without free silicon consisted of large interlocked grains, whereas that of the layers with free silicon showed a cauliflower-like structure and the apparent grain size was small.

The SiC layers examined in the present study were irradiated and post-irradiation examination (PIE) will be started in the near future. This PIE is expected to reveal important relations between the deposition conditions and irradiation behaviour.

Acknowledgement

The authors wish to express their thanks to Dr T. Kondo, Director of Department of Fuels and Materials Research of Japan Atomic Energy Research Institute, for his interest and encouragement.

References

1. R. FÖRTHMANN, E. GYARMATI, J. LINKE and E. WALLURA, *High Temp. High Press.* **14** (1982) 477.
2. R. E. BULLOCK, *J. Nucl. Mater.* **125** (1984) 304.
3. K. MINATO, T. OGAWA, K. FUKUDA, K. IKAWA and K. IWAMOTO, JAERI-M 84-002 (1984).
4. T. N. TIEGS, *Nucl. Technol.* **57** (1982) 389.
5. R. J. LAUF, (ORNL/TM-7393, 1980).
6. R. J. LAUF, T. B. LINDEMER and R. L. PEARSON, *J. Nucl. Mater.* **120** (1984) 6.
7. A. NAOUMIDIS, R. BENZ and J. ROTTMANN, *High Temp. High Press.* **14** (1982) 53.
8. E. GYARMATI and H. NICKEL, (Jül-900-RW, 1972).
9. J. I. FEDERER, *Thin Solid Films* **40** (1977) 89.
10. D. P. STINTON and W. J. LACKEY, *Amer. Ceram. Soc. Bull.* **57** (1978) 568.
11. R. J. LAUF and D. N. BROSKI, ORNL/TM-7571 (1981).
12. E. WALLURA, H. HOVEN, K. KOIZLIK J. LINKE and A. -W. MEHNER, Jül-1871 (1983).
13. P. KRAUTWASSER, G. M. BEGUN and P. ANGELINI, *J. Amer. Ceram. Soc.* **66** (1983) 424.
14. K. MINATO and K. FUKUDA, unpublished data (1987).
15. *Idem, J. Nucl. Mater.* **149** (1987) 233.
16. B. E. WARREN, "X-ray Diffraction" (Addison-Wesley, Massachusetts, 1969) p. 258.
17. H. P. KLUG and L. E. ALEXANDER, "X-ray Diffraction Procedures for Polycrystalline and Amorphous Materials" (Wiley, New York, 1974) p. 618.
18. E. ERBEN and H. HAUSNER, EUR-4946e (1973).
19. E. H. VOICE and V. C. SCOTT, in "Special Ceramics 5", edited by P. Popper (British Ceramic Research Association, 1972) p. 1.
20. T. D. GULDEN, *J. Amer. Ceram. Soc.* **51** (1968) 424.
21. F. HOLUB, SGAE-ME-51/73 (1973).
22. R. WEISS and R. J. DIEFENDORF, in "Silicon Carbide – 1973", edited by B. C. Marshall *et al.* (University of South Carolina Press, South Carolina, 1973) p. 80.

Received 12 May
and accepted 22 July 1987